

# Hybrid Imitation Learning for Real-Time Service Restoration in Resilient Distribution Systems

Yichen Zhang, *Member, IEEE*, Feng Qiu, *Senior Member, IEEE*, Tianqi Hong, *Member, IEEE*,  
Zhaoyu Wang, *Senior Member, IEEE*, Fangxing (Fran) Li, *Fellow, IEEE*

**Abstract**—Self-healing capability is one of the most critical factors for a resilient distribution system, which requires intelligent agents to automatically perform restorative actions online, including network reconfiguration and reactive power dispatch. These agents should be equipped with a predesigned decision policy to meet real-time requirements and handle highly complex  $N - k$  scenarios. The disturbance randomness hampers the application of exploration-dominant algorithms like traditional reinforcement learning (RL), and the agent training problem under  $N - k$  scenarios has not been thoroughly solved. In this paper, we propose the imitation learning (IL) framework to train such policies, where the agent will interact with an expert to learn its optimal policy, and therefore significantly improve the training efficiency compared with the RL methods. To handle tie-line operations and reactive power dispatch simultaneously, we design a hybrid policy network for such a discrete-continuous hybrid action space. We employ the 33-node system under  $N - k$  disturbances to verify the proposed framework.

**Index Terms**—Service restoration, imitation learning, reinforcement learning, deep learning, mixed-integer linear programming, resilient distribution system.

## NOMENCLATURE

### Indices and Sets

$t, \mathcal{T}, T$	index, index set, number of steps
$h, \mathcal{N}_P, N_P$	index, index set, number of point of common coupling
$i/j, \mathcal{N}_B, N_B$	index, index set, number of buses
$k, \mathcal{N}_{SC}, N_{SC}$	index, index set, number of shunt capacitors
$l, \mathcal{N}_L, N_L$	index, index set, number index of lines
$m, \mathcal{N}_S, N_S$	index, index set, number (if countable) of states
$n, \mathcal{N}_A, N_A$	index, index set, number (if countable) of actions

### Continuous Decision Variables

$P_{h,t}^{PCC}$	active power injection at point of common coupling $h$ during step $t$
$Q_{h,t}^{PCC}$	reactive power injection at point of common coupling $h$ during step $t$
$V_{i,t}$	voltage of bus $i$ during step $t$
$Q_{k,t}^{SC}$	reactive power output of shunt capacitor $k$ during step $t$
$P_{l,t}, Q_{l,t}$	active, reactive power flow on line $l$ during step $t$

### Discrete Decision Variables

$u_{l,t}^L$	status of line $l$ during step $t$ : 1 closed and 0 otherwise
-------------	---

$a_{l,t}^T$

action decision of tie-line  $l$  during step  $t$ : 1 to be closed and 0 otherwise

$u_{k,t}^{SC}$

status of shunt capacitor  $k$  during step  $t$ : 1 active and 0 otherwise

$u_{i,t}^D$

connection status of demand at bus  $i$  during step  $t$ : 1 connected and 0 otherwise

$u_{i,j,t}^R$

indication if bus  $i$  is the parent bus of  $j$ : 1 true and 0 false

### Parameters

$P_i^D, Q_i^D$

active, reactive power demand at bus  $i$

$\underline{P}_l, \bar{P}_l$

min, max active power flow of line  $l$

$\underline{Q}_l, \bar{Q}_l$

min, max reactive power flow of line  $l$

$\underline{Q}_k^{SC}, \bar{Q}_k^{SC}$

min, max reactive power output of shunt capacitor  $k$

$\epsilon$

allowable voltage deviation from nominal value

## I. INTRODUCTION

The distribution automation is the fundamental step in the path of smart grids [1]. Given the fact that nearly 90% of all power outages and disturbances have their roots in the distribution network [1], distribution system restoration (DSR), as one of the core functions in distribution automation, builds up the cornerstone of smart grids technologies [2]. The objective of DSR is to search for alternative paths to re-energize the loads in out-of-service areas through a series of switching operations. Typical distribution systems have normally closed sectionalizing switches and normally open tie switches. When a fault is identified, the restoration plan will use tie switches to reconfigure the network so that the disrupted customers can be connected to available feeders [3].

Automatically and promptly conducting *network reconfiguration* is one of the most critical factors for a resilient distribution system. The automation is driven by intelligent devices such as IntelliRupter® [4] as well as intelligent agents, which are computing and logic elements and capable of making decisions. The agent will have a built-in policy mapping from different faulty scenarios to corresponding optimal restorative actions. The policy can be predefined or reactive. The reactive policy requires the agent to solve mathematical programming (MP) online [5]. Although various MP formulations for distribution restorations have been proposed [5]–[15], these technologies needs devices to have sophisticated computational architectures. Furthermore, the solution time may not be able to meet the real-time requirement. Therefore, a predefined or trained policy is more suitable for online and

Y. Zhang, F. Qiu, T. Hong are with Argonne National Laboratory, Lemont, IL 60439 USA (email: thong@anl.gov).

Z. Wang is with Iowa State University, Ames, IA 50011 USA.

F. Li is with University of Tennessee, Knoxville, TN 37996 USA.

real-time applications, which is the scope of this paper as illustrated in Fig. 1.

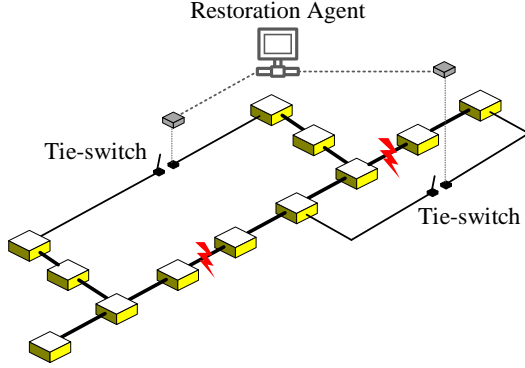


Fig. 1. The scope of this work: training intelligent agent for automatic service restoration through network reconfiguration under random line outages.

If the agent is expected to perform simple tie-line switchings, the built-in policy can be constructed as logic flows with experts' knowledge. Otherwise, the reinforcement learning (RL) problem has been framed for training the agents with optimal restoration policy [16]–[20]. The general technical road map is to first calculate the value of states or state-action pairs offline, that is, training the agent. Then, optimal tie-line operations can be retrieved from the value function with nearly no cost and executed online given observed states. Ref. [16] employed the dynamic programming algorithm to compute the exact value function, which is intractable for high dimensional problems. In Ref. [17], the value function was estimated using the approximate dynamic programming algorithm. Both algorithms, however, require the knowledge of the state transition probabilities, which are difficult to know in advance. The temporal difference learning methods, such as Q-learning, estimate the empirical state transition probabilities from observations. In Refs. [18] and [19], the Q-learning algorithm with the  $\epsilon$ -greed policy was employed to perform offline training such that the agent can reconfigure the network online. Ref. [20] proposed a mixed strategy, in which the online restoration plan either from the agent or an MP was adopted based on certain confident metrics. While in offline mode, the agent was also trained using the Q-learning algorithm.

Despite the innovations, the aforementioned works usually consider a small set of disturbance, and the agent training problem under  $N - k$  scenarios has not been thoroughly solved. This disturbance randomness hampers the application of exploration-dominant algorithms like traditional RL, which is known to converge slowly due to the exploration and exploitation dilemma [21]. In other words, these works rely on random exploration strategies, such as  $\epsilon$ -greed, to locally improve a policy [22]. With additional disturbance randomness, the number of interactions required to learn a policy is enormous, leading to a prohibitive cost. Such a capability limitation on handling disturbance randomness significantly impedes the deployment in real-world scenarios.

To overcome this limitation, the paper proposes the imitation learning (IL) framework for training the restoration agent. The IL framework has recently received attention for its capability to speed up policy learning when solving RL problems in the computer science community [22]–[28]. Unlike pure RL algorithms, IL leverages prior knowledge about a problem in terms of expert demonstrations and train the agents to mimic these demonstrations rather than optimizing a reward function. Its fundamental form consists of training a policy to predict the expert's actions from states in the demonstration data using supervised learning. Here, we leverage well-studied MP-based restoration as the expert. In addition, reconfigured networks may exhibit longer lines and low voltages. Thus, we consider tie-line operations and reactive power dispatch simultaneously to restore more loads. The contribution of this paper is concluded as follows. From the problem-solving perspective:

- We solve the restoration agent training under random  $N - k$  contingencies. The empirical studies reveal that the training complexity is beyond the capability of traditional RL algorithms.
- We consider both tie-line operations and reactive power dispatch, which leads to a hybrid action space.

To address the challenging problem, we improve the state-of-the-art agent training methods by:

- proposing the IL framework to improve training efficiency and reduce the number of agent-environment interactions required to train a policy. We show that the IL algorithms significantly outperform the deep Q-learning under random  $N - k$  contingencies.
- strategically designing MP-based experts and environments with tailored formulations for IL algorithms
- developing a hybrid policy structure and training algorithms to accommodate the mixed discrete and continuous action space

It is worth mentioning that the IL framework acts as a bridge between RL-based techniques and MP-based methods and a way to leverage well-studied MP-based decision-making systems for RL-based automation.

## II. PROBLEM STATEMENT

Let the distribution system be denoted as a graph  $\mathcal{G} = (\mathcal{N}_B, \mathcal{N}_L)$ , where  $\mathcal{N}_B$  denotes all buses (vertices) and  $\mathcal{N}_L$  denotes all lines (edges). The bus set is categorized into substation buses  $\mathcal{N}_{B,S}$  and non-substation buses  $\mathcal{N}_{B,NS}$ . The line set is categorized into non-switchable line set  $\mathcal{N}_{L,NS}$  and tie-line set  $\mathcal{N}_{L,T}$ . The non-switchable lines can not be actively controlled unless tripped due to external disturbances. The status of tie-lines can be controlled through tie-switches to adjust the network configuration.

Assume a  $N_{L,NS} - k$  contingency scenario indicating that  $k$  lines from the set  $\mathcal{N}_{L,NS}$  are tripped. Without loss of generality, we uniformly sample these  $k$  lines from  $\mathcal{N}_{L,NS}$  in each scenario (or episode<sup>1</sup>). Let  $\mathcal{N}_{L,NS}^F$  be the set of faulty lines and  $\mathcal{N}_{L,NS}^{NF}$  be

<sup>1</sup>The terms *scenario* and *episode* are regarded the same in this paper and will be used interchangeably.

the set of non-faulty lines. The goal for a well-trained agent is to control the tie-lines and shunt capacitors to optimally restore interrupted customers given post-fault line status.

To account for the time-dependent process [13], such as the saturating delays of tie-switches and shunt capacitors, as well as reducing transients, we consider a multi-step restoration. In each step, *at most one* tie-line is allowed to operate. In addition, closed tie-lines are not allowed to open again. Meanwhile, all shunt capacitors can be dispatched through all steps. Naturally, we set the step number equal to the number of tie-lines  $N_{L,T}$ . During the restoration process, the network radiality must be maintained, and the tie-line operations that violate the radiality constraint will be denied.

We formalize the above setting using the episodic finite Markov decision process (EF-MDP) [21]. An EF-MDP  $\mathcal{M}$  can be described by a six-tuple  $\mathcal{M} = \langle \mathcal{S}, \mathcal{A}, \mathcal{D}, p(s'|s, a), r(s, a), T \rangle$ , where  $\mathcal{S}$  denotes the state space,  $\mathcal{A}$  denotes the action space,  $\mathcal{D}$  denotes the disturbance space,  $p(s'|s, a)$  denotes the state transition probability,  $r$  denotes the real-valued reward function,  $T$  denotes the number of steps in each episode, and  $s', s \in \mathcal{S}$ ,  $a \in \mathcal{A}$ . The action space is hybrid, consisting of a discrete action space  $\mathcal{A}_T$  for tie-line operations and a continuous action space  $\mathcal{A}_C$  where

$$\mathcal{A}_T = [0, 1, \dots, N_{L,T}] \quad (1)$$

$$\mathcal{A}_C = [\underline{Q}_1^C, \bar{Q}_1^C] \cup \dots \cup [\underline{Q}_{N_C}^C, \bar{Q}_{N_C}^C] \quad (2)$$

A trajectory can be denoted as

$$\tau = (s_0(d), a_1, s_1, a_2, s_2, \dots, a_T, s_T) \quad (3)$$

where  $s_0(d)$ , or  $s_0$  for short, is the initial faulty condition due to disturbance  $d \in \mathcal{D}$ . For actions that violate the radiality constraint, the corresponding transition probability will be zero and one otherwise.

### III. DEEP IMITATION LEARNING

#### A. Imitation Learning Problem

The IL training process aims to search for a policy  $\pi(a|s)$  (a conditional distribution of action  $a \in \mathcal{A}$  given state  $s \in \mathcal{S}$ ) from the class of policies  $\Pi$  to mimic the expert policy  $\pi^*$ . The expert policy is assumed to be deterministic. Without loss of generality, consider a countable state space  $\mathcal{S} = [s^1, s^2, \dots, s^{N_S}]$  with  $N_S$  number states. Let  $\rho_0$  denote the initial distribution of states and  $\rho_0(s^m)$  denote the probability of state  $s^m$ . Let  $\rho_t^\pi$  denote the distribution of states at time  $t$  if the agent executes the policy  $\pi$  from step 1 to  $t - 1$ . The law of  $\rho_t^\pi$  can be computed recursively as follows

$$\rho_t^\pi(s^m) = \sum_{s_{t-1} \in \mathcal{S}} \rho_{t-1}(s_{t-1}) \sum_{a_t \in \mathcal{A}} \pi(a_t|s_{t-1}) p(s_t^m|s_{t-1}, a_t) \quad (4)$$

Then, the average distribution of states is defined as  $\bar{\rho}^\pi(s) = \sum_{t=1}^T \rho_{t-1}^\pi(s)/T$ , which represents the state visitation frequency over  $T$  time steps if policy  $\pi$  is employed.

The 0-1 loss of executing action  $a$  in state  $s$  with respect to (w.r.t) the expert policy  $\pi^*$  is denoted as follows

$$e(s, a) = I(a \neq \pi^*(s)) \quad (5)$$

where  $I(\bullet)$  is the indicator function. The expected 0-1 loss of policy  $\pi$  in state  $s$  reads as follows

$$e_\pi(s) = \mathbb{E}_{a \sim \pi_s} [e(s, a)] \quad (6)$$

The expected  $T$ -step loss w.r.t  $\pi$  is

$$L(\pi) = \mathbb{E}_{s \sim \rho^\pi} [e_\pi(s)] \quad (7)$$

The goal is to find a policy  $\bar{\pi}$  that minimize the expected  $T$ -step loss  $L(\pi)$ , that is,

$$\bar{\pi} = \operatorname{argmin}_{\pi \in \Pi} L(\pi) = \operatorname{argmin}_{\pi \in \Pi} \mathbb{E}_{s \sim \rho^\pi} [e_\pi(s)] \quad (8)$$

Note that this objective function is non-convex due to the dependence between the objective parameter  $\rho^\pi$  and the decision space  $\Pi$ .

#### B. Imitation Learning Algorithm

The most effective form of imitation learning is behavior cloning (BC). In the BC algorithm summarized, trajectories are collected under the expert's policy  $\pi^*$ , and the IL problem renders to a supervised learning problem, where the states are the features and the actions are the labels. The objective of BC reads as follows

$$\bar{\pi} = \operatorname{argmin}_{\pi \in \Pi} \mathbb{E}_{s \sim \rho^{\pi^*}} [e_\pi(s)] \quad (9)$$

The objective in Eq. (9) disassociates the dependency between the objective parameter and the decision space. The BC algorithm is described in Algorithm 1. Several major functions are explained as follows.

- **Expert:** Since we are addressing a multi-period scheduling problem, it is difficult to directly obtain an expert mapping  $\pi^*$ . Therefore, a mixed-integer program (MIP) is employed to obtain the optimal actions. This MIP is specified as an expert solver  $\text{Expert}(s_{t-1}, [t, \dots, T])$ , which takes the initial state at  $t-1$  and the scheduling interval  $[t, \dots, T]$ , and return the optimal actions  $a_t, \dots, a_T$ . The detailed MIP formulation is given in Section IV.
- **Act:** The DSR environment interacts with the policy through **Act**. Given a disturbance  $d$ , total step  $T$ , and the policy (either the mapping or expert solver), **Act** returns a  $T$ -step trajectory. More details are described in Algorithm 2.
- **Eval:** **Eval** compares the learned policy-induced trajectory with the optimal one and calculates the ratio  $r$  between restored total energy under the learned policy and the optimal restored total energy. The ratio is defined as the performance score of the learned policy in each iteration.

Algorithm 2 runs either the learned policy or the expert solver on the DSR environment **Env** to obtain the trajectory. The DSR environment **Env** is built on the standard Open-AI Gym environment template [29]. There are two major functions: **Env.Reset** and **Env.Step**. The function **Env.Reset** initializes the system status with a given disturbance. **Env.Step** determines the system best next-step status under a given action. To do so, another MIP is formulated inside **Env.Step** and will be described in Section IV.

**Algorithm 1: Behavior cloning (BC)**


---

**input** : expert solver  $\text{Expert}$ , deep neural net policy  $\bar{\pi}$ , neural network training function  $\text{Train}(\cdot, \cdot, \cdot)$ , environment interaction  $\text{Act}(\cdot, \cdot, \cdot)$ , disturbance set  $\mathcal{D}$ , stochastic sampling function  $\text{Sample}(\cdot)$ , policy evaluation function  $\text{Eval}(\cdot, \cdot)$

```

1  $X \leftarrow \emptyset$  // initialize the input
2  $Y \leftarrow \emptyset$  // initialize the label
3  $P \leftarrow \emptyset$  // initialize the performance
4  $\bar{\pi}^1 \in \Pi$  // initialize the policy
5 for  $i \leftarrow 1$  to  $N$  do
6    $d \leftarrow \text{Sample}(\mathcal{D})$ 
7    $(s_0, a_1, s_1, \dots, a_T, s_T) \leftarrow \text{Act}(d, T, \text{Expert})$ 
8    $X \leftarrow X \cup (s_0, \dots, s_{T-1})$ 
9    $Y \leftarrow Y \cup (a_1, \dots, a_T)$ 
10   $\bar{\pi}^{i+1} \leftarrow \text{Train}(X, Y, \bar{\pi}^i)$ 
11   $d \leftarrow \text{Sample}(\mathcal{D})$ 
12   $r \leftarrow \text{Eval}(\text{Act}(d, T, \text{Expert}), \text{Act}(d, T, \bar{\pi}^{i+1}))$ 
13   $P \leftarrow P \cup (d, r)$ 
14 end
output: Trained deep neural net  $\bar{\pi}$ , performance scores  $P$ 

```

---

**Algorithm 2: Environment interaction  $\text{Act}$** 


---

**input** : disturbance  $d$ , time step  $T$ , policy function or expert solver  $f$ , DSR environment  $\text{Env}$

```

1  $s_0 \leftarrow \text{Env.Reset}(d)$ 
2 if  $f == \text{Expert}$  then
3   /* run Env under the expert policy */
4    $(a_1, \dots, a_T) \leftarrow \text{Expert}(s_0, [1, \dots, T])$ 
5   for  $t \leftarrow 1$  to  $T$  do
6      $s_t \leftarrow \text{Env.Step}(a_t)$ 
7   end
8 if  $f == \pi$  then
9   /* run Env under learned policy */
10  for  $t \leftarrow 1$  to  $T$  do
11     $a_t \leftarrow \pi(s_{t-1})$ 
12     $s_t \leftarrow \text{Env.Step}(a_t)$ 
13  end
output:  $T$ -step trajectory  $(s_0, a_1, s_1, \dots, a_T, s_T)$ 

```

---

**C. Hybrid Policy**

The training in Algorithm 1 Line 10 is a multi-class classification problem, which is not able to handle continuous action spaces. Thus, Algorithm 1 can only be used for automatic tie-line operators. To simultaneously coordinate tie-line operations and reactive power dispatch, we propose a hybrid policy network, as shown in Fig. 2. The action spaces of the hybrid neural network are mixed continuous and discrete. At the higher level, there is a single neural network to predict the optimal tie-line actions given measured states. Each tie-line

action is associated with a neural network for reactive power dispatch. The dispatch ranges associated with individual tie-lines can be a subset or entire continuous action spaces. Considering the fact that under each tie-line operation, the system may admit a different power flow pattern, we attach the entire dispatch spaces in each tie-line action. It is also worth mentioning that the states for predicting discrete and continuous actions can be different.

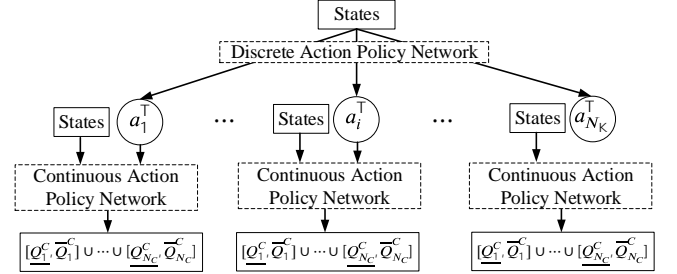


Fig. 2. Discrete-continuous hybrid policy network.

The training process for the hybrid policy network is described in Algorithm 3. The additional effort from Algorithm 1 is that we will train reactive power dispatchers under each tie-line action. To do this, we first initialize the dispatcher training dataset as shown in Line 2. In each episode, we group the dispatch commands from the expert  $\text{hExp}$  based on the tie-line actions as shown in Lines 11 and 12. The final step in each episode is to train the classifier and regressors, respectively, as shown in Lines 14 and 15. The hybrid behavior cloning algorithm will interact with the environment that includes both tie-line and var dispatch, which is described in Algorithm 4. Algorithm 4 is similar to Algorithm 2 except that the hybrid actions are generated using the hybrid policy as shown in Lines 10 and 11, and the DSR environment has hybrid actions. The MIP formulation of  $\text{hEnv}$  will be introduced in Section IV.

**IV. MATHEMATICAL PROGRAMMING-BASED EXPERT AND ENVIRONMENT**

This section describes the MIP formulation for  $\text{Expert}$  and  $\text{hExp}$ . We will first introduce generic constraints for the DSR problem and formulate the two problems with different constraints.

Let  $\mathcal{L}(\cdot, i)$  denote the set of lines for which bus  $i$  is the to-bus, and  $\mathcal{L}(i, \cdot)$  denote the set of lines for which bus  $i$  is the from-bus. Let  $\mu(l)$  and  $\nu(l)$  map from the index of line  $l$  to the index of its from-bus and to-bus, respectively. The nature of radiality guarantees that  $\mu(l)$  and  $\nu(l)$  are one-to-one mappings. Let  $\mathcal{P}$  map from the index of bus  $i$  to the substation index. Without loss of generality, we consider one active substation and assume Bus 1 is connected to it. Let  $\mathcal{C}$  map from the index of bus  $i$  to the shunt capacitor. Let  $\mathcal{T} = [t_0, t_1, \dots, T]$  be the step index and  $t \in \mathcal{T}$ .

Following the convention in [30] and [11], linearized disflow equations are employed to represent power flows and



**Algorithm 3: Hybrid behavior cloning (HBC)**


---

**input :** hybrid action expert solver  $\text{hExp}$ , tie-line operation policy  $\bar{\pi}$ , reactive power dispatch policy under tie-line action  $k$   $\bar{\pi}_k$ , classifier training function  $\text{TrainClf}(\cdot, \cdot, \cdot)$ , regressors training function  $\text{TrainReg}(\cdot, \cdot, \cdot)$ , hybrid action environment interaction  $\text{hAct}(\cdot, \cdot, \cdot)$ , disturbance set  $\mathcal{D}$ , stochastic sampling function  $\text{Sample}(\cdot)$ , policy evaluation function  $\text{Eval}(\cdot, \cdot)$

- 1  $X \leftarrow \emptyset, Y \leftarrow \emptyset$
- 2  $X_k \leftarrow \emptyset, Y_k \leftarrow \emptyset$
- 3  $P \leftarrow \emptyset$
- 4  $\bar{\pi}^1 \in \Pi, \bar{\pi}_k^1 \in \Pi$
- 5 **for**  $i \leftarrow 1$  **to**  $N$  **do**
- 6      $d \leftarrow \text{Sample}(\mathcal{D})$
- 7      $(s_0, a_1^D, a_1^C, s_1, \dots, a_T^D, a_T^C, s_T) \leftarrow \text{hAct}(d, T, \text{hExp})$
- 8      $X \leftarrow X \cup (s_0, \dots, s_{T-1})$
- 9      $Y \leftarrow Y \cup (a_1^D, \dots, a_T^D)$
- 10    **for**  $t \leftarrow 1$  **to**  $T$  **do**
- 11        $X_{a_t^D} \leftarrow X_{a_t^D} \cup s_{t-1}$
- 12        $Y_{a_t^D} \leftarrow Y_{a_t^D} \cup a_t^C$
- 13    **end**
- 14     $\bar{\pi}^{i+1} \leftarrow \text{TrainClf}(X, Y, \bar{\pi}^i)$
- 15     $\bar{\pi}_k^{i+1} \leftarrow \text{TrainReg}(X_k, Y_k, \bar{\pi}_k^i)$
- 16     $d \leftarrow \text{Sample}(\mathcal{D})$
- 17     $r \leftarrow \text{Eval}(\text{hAct}(d, T, \text{hExp}), \text{hAct}(d, T, (\bar{\pi}^{i+1}, \bar{\pi}_k^{i+1})))$
- 18     $P \leftarrow P \cup (d, r)$
- 19 **end**

**output:** Trained tie-line operator  $\bar{\pi}$ , trained reactive power dispatcher  $\bar{\pi}_k$ , performance scores  $P$

---

**Algorithm 4: Hybrid action environment interaction**  
 $\text{hAct}$ 


---

**input :** disturbance  $d$ , time step  $T$ , policy function or expert solver  $f$ , hybrid-action DSR environment  $\text{hEnv}$

- 1  $s_0 \leftarrow \text{hEnv.Reset}(d)$
- 2 **if**  $f == \text{hExp}$  **then**
- 3      $(a_1^D, a_1^C, \dots, a_T^D, a_T^C) \leftarrow \text{hExp}(s_0, [1, \dots, T])$
- 4     **for**  $t \leftarrow 1$  **to**  $T$  **do**
- 5        $s_t \leftarrow \text{hEnv.Step}((a_t^D, a_t^C))$
- 6     **end**
- 7 **end**
- 8 **if**  $f == (\pi, \pi_k)$  **then**
- 9     **for**  $t \leftarrow 1$  **to**  $T$  **do**
- 10        $a_t^D \leftarrow \pi(s_{t-1})$
- 11        $a_t^C \leftarrow \pi_{a_t^D}(s_{t-1})$
- 12        $s_t \leftarrow \text{hEnv.Step}((a_t^D, a_t^C))$
- 13     **end**
- 14 **end**

**output:**  $T$ -step trajectory  $(s_0, a_1^D, a_1^C, s_1, \dots, a_T^D, a_T^C, s_T)$

---

voltages in the network and are described as follows

$$\begin{aligned}
 \sum_{\forall l \in \mathcal{L}(\cdot, i)} P_{l,t} + \sum_{\forall h \in \mathcal{P}(i)} P_{h,t}^{\text{PCC}} \\
 &= \sum_{\forall l \in \mathcal{L}(i, \cdot)} P_{l,t} + u_{i,t}^D P_{i,t}^D \quad \forall i, \forall t \\
 \sum_{\forall l \in \mathcal{L}(\cdot, i)} Q_{l,t} + \sum_{\forall h \in \mathcal{P}(i)} Q_{h,t}^{\text{PCC}} + \sum_{\forall k \in \mathcal{C}(i)} Q_{k,t}^{\text{SC}} \\
 &= \sum_{\forall l \in \mathcal{L}(i, \cdot)} Q_{l,t} + u_{i,t}^D Q_{i,t}^D \quad \forall i, \forall t
 \end{aligned} \tag{10}$$

The line flow should respect the limits, which will be enforced to be zero if it is opened

$$\begin{aligned}
 u_{l,t}^L \underline{P}_l &\leq P_{l,t} \leq u_{l,t}^L \bar{P}_l \quad \forall l, \forall t \\
 u_{l,t}^L \underline{Q}_l &\leq Q_{l,t} \leq u_{l,t}^L \bar{Q}_l \quad \forall l, \forall t
 \end{aligned} \tag{11}$$

The shunt capacitor should also respect the limits, which will be enforced to be zero if it is opened

$$u_{k,t}^{\text{SC}} \underline{Q}_k^{\text{SC}} \leq Q_{k,t}^{\text{SC}} \leq u_{k,t}^{\text{SC}} \bar{Q}_k^{\text{SC}} \quad \forall l, \forall t \tag{12}$$

The linear relation between voltages and line flow needs to be enforced when the line  $l$  is closed

$$\begin{aligned}
 (u_{l,t}^L - 1)M &\leq V_{\nu(l),t} - V_{\mu(l),t} + \frac{R_l P_{l,t} + X_l Q_{l,t}}{V_1} \quad \forall l, \forall t \\
 (1 - u_{l,t}^L)M &\geq V_{\nu(l),t} - V_{\mu(l),t} + \frac{R_l P_{l,t} + X_l Q_{l,t}}{V_1} \quad \forall l, \forall t
 \end{aligned} \tag{13}$$

The voltages should be maintained within permissible ranges

$$1 - \epsilon \leq V_{i,t} \leq 1 + \epsilon \quad \forall i, \forall t \tag{14}$$

The radiality constraints are expressed as follows [31]

$$\begin{aligned}
 u_{\mu(l),\nu(l),t}^R + u_{\nu(l),\mu(l),t}^R &= u_{l,t}^L \quad \forall l, \forall t \\
 u_{i,j,t}^R &= 0 \quad \forall i, \forall j \in \mathcal{N}_{B,S}, \forall t \\
 \sum_{i \in \mathcal{N}_B} u_{i,j,t}^R &\leq 1 \quad \forall j, \forall t
 \end{aligned} \tag{15}$$

Within all non-switchable lines  $\mathcal{N}_{L,NS}$ , the status of faulty lines  $\mathcal{N}_{L,NS}^F$  is enforced to be zero and the status of non-faulty lines  $\mathcal{N}_{L,NS}^{NF}$  is enforced to be one

$$\begin{aligned}
 u_{l,t}^L &= 0 \quad \forall l \in \mathcal{N}_{L,NS}^F, \forall t \\
 u_{l,t}^L &= 1 \quad \forall l \in \mathcal{N}_{L,NS}^{NF}, \forall t
 \end{aligned} \tag{16}$$

For a multi-step scenario, the restored loads are not allowed to be disconnected again

$$u_{i,t}^D \geq u_{i,t-1}^D \quad \forall i, \forall t \setminus \{t_0\} \tag{17}$$

Similarly, closed tie-lines cannot be opened

$$u_{l,t}^L \geq u_{l,t-1}^L \quad \forall l \in \mathcal{N}_{L,T}, \forall t \setminus \{t_0\} \tag{18}$$

In addition, only one tie-line can be operated in one step

$$\sum_{l \in \mathcal{N}_{L,T}} u_{l,t}^L - \sum_{l \in \mathcal{N}_{L,T}} u_{l,t-1}^L \leq 1 \quad \forall t \setminus \{t_0\} \tag{19}$$

And all tie-lines are equal to the initial values

$$u_{l,t_0}^L = \hat{u}_l^L \quad \forall l \in \mathcal{N}_{L,T} \tag{20}$$

In some instances, there will be multiple shunt capacitor dispatch solutions for an optimal load restoration, and the shunt dispatch results will jumpy between these solutions in an episode. This will jeopardize a smooth learning process. Therefore, a set of constraints is considered to limit the dispatch frequency

$$M(1 - z_{k,t}) \leq Q_{k,t}^{\text{SC}} - Q_{k,t-1}^{\text{SC}} \quad (21a)$$

$$-M(1 - z_{k,t}) \leq \Delta_{k,t}^{\text{SC}} - (Q_{k,t}^{\text{SC}} - Q_{k,t-1}^{\text{SC}}) \quad (21b)$$

$$M(1 - z_{k,t}) \geq \Delta_{k,t}^{\text{SC}} - (Q_{k,t}^{\text{SC}} - Q_{k,t-1}^{\text{SC}}) \quad (21c)$$

$$-Mz_{k,t} \leq \Delta_{k,t}^{\text{SC}} + (Q_{k,t}^{\text{SC}} - Q_{k,t-1}^{\text{SC}}) \quad (21d)$$

$$Mz_{k,t} \geq \Delta_{k,t}^{\text{SC}} + (Q_{k,t}^{\text{SC}} - Q_{k,t-1}^{\text{SC}}) \quad (21e)$$

$$\forall k, \forall t \in \mathcal{T} \quad (21f)$$

where we introduce two slack variables:  $\Delta_{k,t}^{\text{SC}}$  is a continuous variable to express the incremental changes of shunt capacitor  $k$  from time  $t-1$  to  $t$ , and  $z_{k,t}$  is a binary variable to denote if there exists incremental changes of shunt capacitor  $k$  from time  $t-1$  to  $t$ . Eq. (21a) enforces  $z_{k,t}$  to be one if  $Q_{k,t}^{\text{SC}}$  and  $Q_{k,t-1}^{\text{SC}}$  are different, where  $M$  is a big positive number. Eqs. (21b)-(21e) ensure that  $\Delta_{k,t}^{\text{SC}}$  equals to  $Q_{k,t}^{\text{SC}} - Q_{k,t-1}^{\text{SC}}$  if  $z_{k,t}$  is one, and  $\Delta_{k,t}^{\text{SC}}$  equals to zero when  $z_{k,t}$  is zero. With the set of constraints,  $\Delta_{k,t}^{\text{SC}}$  precisely denotes the incremental changes and can be minimized in the objective function.

The expert solver `Expert` takes the disturbance  $d$  (the set of faulty lines  $\mathcal{N}_{\text{L,NS}}^{\text{F}}$ ), the initial tie-line status  $\hat{u}_l^{\text{T}}$ , where  $\forall l \in \mathcal{N}_{\text{L,T}}$ , and the step index  $\mathcal{T} = [t_0, t_1, \dots, T]$  as inputs and solver the following MIP problem

$$\max \sum_t \sum_i u_{i,t}^{\text{D}} P_i^{\text{D}} \quad (22a)$$

$$\text{subject to (10) - (20)} \quad \forall t \in \mathcal{T} \quad (22b)$$

$$u_{k,t}^{\text{SC}} = 0 \quad \forall k, \forall t \in \mathcal{T} \quad (22c)$$

where (22c) deactivate shunt capacitors since they will not be considered in `Expert`. The solution will provide a series of tie-line status  $u_{l,t_0}^{\text{T}}, u_{l,t_1}^{\text{T}}, \dots, u_{l,T}^{\text{T}}$  for  $l \in \mathcal{N}_{\text{L,T}}$ . Then, the optimal tie-line operating actions can be parsed as  $a_{t_1}^{\text{T}}, \dots, a_T^{\text{T}}$ . The `Env.Reset` function computes the system initial condition given a random generated faulty line set  $\mathcal{N}_{\text{L,NS}}^{\text{F}}$

$$\max \sum_t \sum_i u_{i,t}^{\text{D}} P_i^{\text{D}} \quad (23a)$$

$$\text{subject to (10) - (16)} \quad \forall t \in [t_0] \quad (23b)$$

$$u_{l,t_0}^{\text{T}} = 0 \quad \forall l \in \mathcal{N}_{\text{L,T}} \quad (23c)$$

$$u_{k,t_0}^{\text{SC}} = 0 \quad \forall k \quad (23d)$$

where Eq. (23c) ensures no tie-line actions under this initial stage. The `Env.Step` aims to restore the maximal load given the disturbance, a tie-line status and the load status from the previous step by solving the following problem

$$\max \sum_t \sum_i u_{i,t}^{\text{D}} P_i^{\text{D}} \quad (24a)$$

$$\text{subject to (10) - (16), (20)} \quad \forall t \in [t_\tau] \quad (24b)$$

$$u_{t_\tau}^{\text{D}} \geq \hat{u}_{t_\tau-1}^{\text{D}} \quad (24c)$$

$$u_{k,t_\tau}^{\text{SC}} = 0 \quad \forall k, \forall t \quad (24d)$$

where  $\hat{u}_{t_\tau-1}^{\text{D}}$  is the load status from the previous step, and Eq. (24c) ensures the restored load will not be disconnected again.

Similarly, hybrid-action expert solver `hExp` solves the following MIP

$$\max \sum_t \left( \sum_i u_{i,t}^{\text{D}} P_i^{\text{D}} + w \sum_k \Delta_{k,t}^{\text{SC}} \right) \quad (25a)$$

$$\text{subject to (10) - (21)} \quad \forall t \in \mathcal{T} \quad (25b)$$

where  $w$  is the weighting factor. The hybrid-action DSR environment `hEnv` also consider the reactive power dispatch. The `hEnv.Reset` function computes the system initial condition given a random generated faulty line set  $\mathcal{N}_{\text{L,NS}}^{\text{F}}$

$$\max \sum_t \sum_i u_{i,t}^{\text{D}} P_i^{\text{D}} \quad (26a)$$

$$\text{subject to (10) - (16)} \quad \forall t \in [t_0] \quad (26b)$$

$$u_{l,t_0}^{\text{L}} = 0 \quad \forall l \in \mathcal{N}_{\text{L,T}} \quad (26c)$$

$$Q_{k,t_0}^{\text{SC}} = 0 \quad \forall k \quad (26d)$$

where Eqs. (26c) and (26d) ensure no restorative actions under this initial stage. The `hEnv.Step` aims to restore the maximal load given the disturbance, a tie-line status and the load status from the previous step by solving the following problem

$$\max \sum_t \sum_i u_{i,t}^{\text{D}} P_i^{\text{D}} \quad (27a)$$

$$\text{subject to (10) - (16), (20)} \quad \forall t \in [t_\tau] \quad (27b)$$

$$u_{t_\tau}^{\text{D}} \geq \hat{u}_{t_\tau-1}^{\text{D}} \quad (27c)$$

$$Q_{k,t_\tau}^{\text{SC}} = \hat{Q}^{\text{SC}} \quad \forall k \quad (27d)$$

where  $\hat{u}_{t_\tau-1}^{\text{D}}$  is the load status from the previous step, and  $\hat{Q}^{\text{SC}}$  is the var dispatch command.

## V. CASE STUDY

The 33-node system in [32] will be employed in this paper. It is a radial 12.66 kV distribution network, shown in Fig. 3. Detailed network data can be found in [32]. In this system, there are five tie-lines, which are assumed to be opened in the initial phase. Six shunt capacitors are assumed to be deployed in the gray nodes Fig. 3. The dispatch ranges of all shunt capacitors are from -0.2 to 0.2 MVar. In the numerical experiments, we consider three metrics to evaluate the learning performance: (1) *Restoration ratio*: the ratio between the restored load by the agent and the optimal restorable load by the expert in each episode; (2) *Success rate*: number of times that the agent achieves optimal restorable load in  $T$  episodes; (3) *Restoration value*: total restored load by the agent in each episode. The optimization is formulated using Pyomo [33] and solved using IBM ILOG CPLEX 12.8. The deep learning model is built using TensorFlow r1.14.

### A. Policy Network and Feature Selection

Based on the system structure, the policy networks are shown in Fig. 4. The tie-line operation policy network consists of three hidden layers. We use the rectifier linear units (`relu`) as our activation functions. The feature inputs are line status.

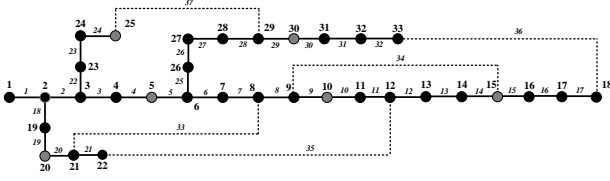


Fig. 3. The 33-node system with five tie-lines. The gray nodes are assumed to be equipped with shunt capacitors.

The shunt capacitor policy network has four hidden layers. For this network, we compare three different feature inputs and two types of activation functions.

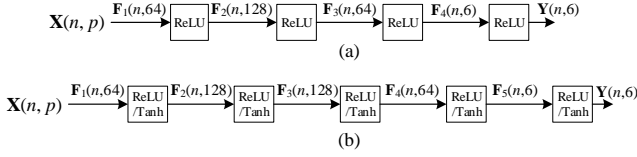


Fig. 4. Deep neural network based policy networks. (a) Tie-line operation policy network. (b) Shunt capacitor dispatch policy network.

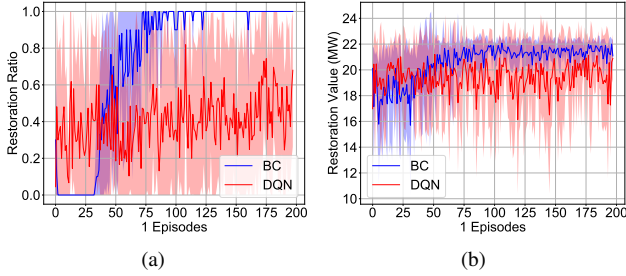


Fig. 5. Training performance of imitation learning-behavior cloning algorithm and reinforcement learning-deep Q network under the  $N - 1$  scenario. (a) Restoration ratio. (b) Restoration value.

### B. IL v.s. RL

In this subsection, we compare the imitation learning Algorithms 1 with an RL baseline algorithm, Deep Q-Network (DQN). We consider only the tie-line actions under the  $N - 1$  random contingency. The restoration ratio and value are shown in Fig. 5 (a) and (b), respectively. As shown, the BC algorithm is able to optimally restore the system after 75 episodes of training, while DQN admits only an averaged 40% restoration ratio over the 200 episodes and is not converging. The problem complexity due to the topology switching is intractable for algorithms that heavily rely on exploration like traditional RL.

### C. Random $N-1$ Contingency

In this subsection, we train the hybrid policy network under the random  $N - 1$  contingency. The training episode is 200. In the var dispatch policy network, we consider three feature inputs: line status, load status and real-valued power flow. We also employ two different activation functions: `relu` and

`tanh`. The training performance is illustrated in Fig. 6. All three metrics are averaged within five steps. We expect that BC has a higher ratio and success rate since the task only involves discrete actions and relatively easier. But with var dispatch capability, the hybrid agent is able to restore approximately 2 MW load in each episode as shown in Fig. 6 (c). The `tanh` is more effective for approximating the var dispatch commands in HBC than `relu`. The reason would be that `tanh` has ranges in both positive and negative real values and is differentiable. As for the features, real-valued power flow slightly outperforms the load status.

### D. Random $N-2$ Contingency

We consider a more complicated random  $N - 2$  scenario and train both BC and HBC agents for 2000 episodes. In this scenario, BC is able to perform optimal restoration around the 500th episode, while HBC is at a much earlier stage, that is, the 200th episode, as shown in Fig. 7. This is owed to the var dispatch capability. After 400 episodes, the success rate of BC is higher than HBC since it handles a simpler task. But under the random  $N - 2$  scenario, BC is also not able to achieve a 100% success rate. This may be related to the feature extraction capability of policy networks and will be investigated in the future. Nevertheless, Fig. 7 (c) shows that the HBC agent can restore 3 MW more in each episode, indicating that it is critical to have var support in the resilient setting. The reason lies in the fact that the reconfigured network may have longer feeders when there are more line outages. Therefore, the voltage drops along reconfigured feeders are more significant.

## VI. CONCLUSIONS AND FUTURE WORKS

In this paper, we propose the IL framework and HBC algorithm for training intelligent agents to perform online service restoration. We strategically design the MIP-based experts, who are able to provide optimal restoration actions for the agent to imitate, and a series of MIP-based environments that agents can interact with. Agents that are trained under the proposed framework can master the restoration skills faster and better compared with RL methods. The agent can perform optimal tie-line operations to reconfigure the network and simultaneously dispatch reactive power of shunt capacitors using the trained policy network. The decision-making process has negligible computation costs and can be readily deployed for online applications. Future efforts will be devoted to feature extraction capability considering unique power network structure as well as a multi-agent training paradigm.

## REFERENCES

- [1] H. Farhangi, "The path of the smart grid," *IEEE Power Energy Mag.*, vol. 8, no. 1, pp. 18–28, 2010.
- [2] A. Zidan and E. F. El-Saadany, "A cooperative multiagent framework for self-healing mechanisms in distribution systems," *IEEE Trans. Smart Grid*, vol. 3, no. 3, pp. 1525–1539, 2012.
- [3] A. Zidan *et al.*, "Fault Detection, Isolation, and Service Restoration in Distribution Systems: State-of-the-Art and Future Trends," *IEEE Trans. Smart Grid*, vol. 8, no. 5, pp. 2170–2185, 2017.
- [4] S. Electric, "Intellirupter® pulsecloser® fault interrupter," S&C Electric Company, Chicago, IL, USA, Tech. Rep., 2019.

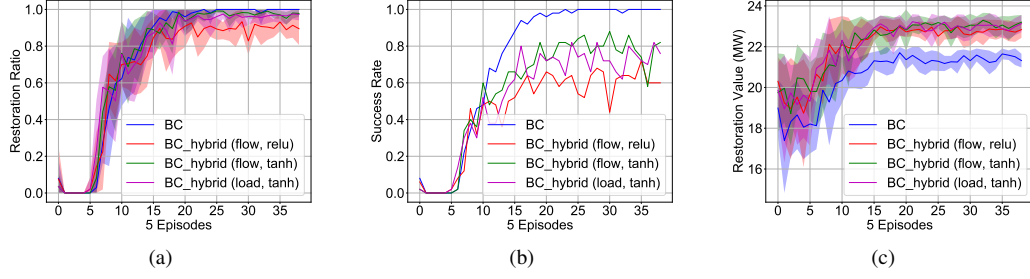


Fig. 6. Training performance of behavior cloning and hybrid behavior cloning under the  $N-1$  scenario. (a) Restoration ratio. (b) Restoration value.

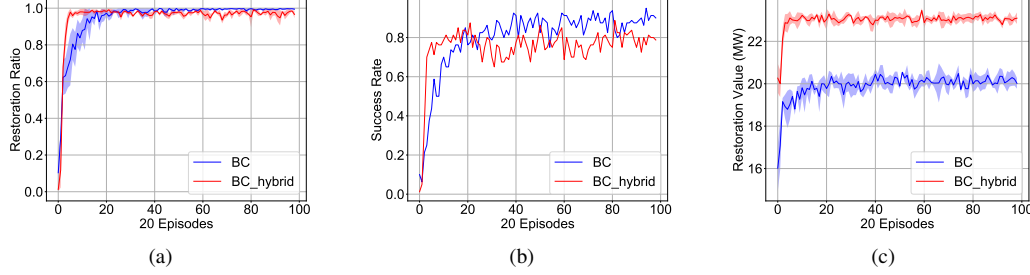


Fig. 7. Training performance of behavior cloning and hybrid behavior cloning under the  $N-2$  scenario. (a) Restoration ratio. (b) Restoration value.

- [5] F. Shariatzadeh, N. Kumar, and A. K. Srivastava, "Optimal control algorithms for reconfiguration of shipboard microgrid distribution system using intelligent techniques," *IEEE Trans. Ind. Appl.*, vol. 53, no. 1, pp. 474–482, 2017.
- [6] S. Khushalani, J. M. Solanki, and N. N. Schulz, "Optimized restoration of unbalanced distribution systems," *IEEE Trans. Power Syst.*, vol. 22, no. 2, pp. 624–630, 2007.
- [7] Z. Wang and J. Wang, "Self-Healing Resilient Distribution Systems Based on Sectionalization into Microgrids," *IEEE Trans. Power Syst.*, vol. 30, no. 6, pp. 3139–3149, 2015.
- [8] H. Gao, Y. Chen, Y. Xu, and C. C. Liu, "Resilience-Oriented Critical Load Restoration Using Microgrids in Distribution Systems," *IEEE Trans. Smart Grid*, vol. 7, no. 6, pp. 2837–2848, 2016.
- [9] Y. Xu *et al.*, "Microgrids for service restoration to critical load in a resilient distribution system," *IEEE Trans. Smart Grid*, vol. 9, no. 1, pp. 426–437, 2018.
- [10] B. Chen, C. Chen, J. Wang, and K. L. Butler-Purry, "Multi-time step service restoration for advanced distribution systems and microgrids," *IEEE Trans. Smart Grid*, vol. 9, no. 6, pp. 6793–6805, 2018.
- [11] A. Arif, Z. Wang, J. Wang, and C. Chen, "Power distribution system outage management with co-optimization of repairs, reconfiguration, and DG dispatch," *IEEE Trans. Smart Grid*, vol. 9, no. 5, pp. 4109–4118, 2018.
- [12] R. Roofegari Nejad and W. Sun, "Distributed Load Restoration in Unbalanced Active Distribution Systems," *IEEE Trans. Smart Grid*, vol. 10, no. 5, pp. 5759–5769, sep 2019.
- [13] H. Sekhavatmanesh and R. Cherkaoui, "A Multi-Step Reconfiguration Model for Active Distribution Network Restoration Integrating the DG Start-Up Sequences," *IEEE Trans. Sustain. Energy*, vol. 3029, no. c, pp. 1–1, 2020.
- [14] W. Li *et al.*, "A Full Decentralized Multi-Agent Service Restoration for Distribution Network with DGs," *IEEE Trans. Smart Grid*, vol. 11, no. 2, pp. 1100–1111, 2020.
- [15] F. Shen *et al.*, "Distributed Self-Healing Scheme for Unbalanced Electrical Distribution Systems Based on Alternating Direction Method of Multipliers," *IEEE Trans. Power Syst.*, vol. 35, no. 3, pp. 2190–2199, 2020.
- [16] R. Pérez-Guerrero *et al.*, "Optimal restoration of distribution systems using dynamic programming," *IEEE Trans. Power Deliv.*, vol. 23, no. 3, pp. 1589–1596, 2008.
- [17] C. Wang *et al.*, "Markov Decision Process-Based Resilience Enhancement for Distribution Systems: An Approximate Dynamic Programming Approach," *IEEE Trans. Smart Grid*, vol. 11, no. 3, pp. 2498–2510, 2020.
- [18] D. Ye, M. Zhang, and D. Sutanto, "A hybrid multiagent framework with Q-learning for power grid systems restoration," *IEEE Trans. Power Syst.*, vol. 26, no. 4, pp. 2434–2441, 2011.
- [19] S. Das *et al.*, "Dynamic reconfiguration of shipboard power systems using reinforcement learning," *IEEE Trans. Power Syst.*, vol. 28, no. 2, pp. 669–676, may 2013.
- [20] M. J. Ghorbani, M. A. Choudhry, and A. Feliachi, "A multiagent design for power distribution systems automation," *IEEE Trans. Smart Grid*, vol. 7, no. 1, pp. 329–339, 2016.
- [21] R. S. Sutton and A. G. Barto, *Reinforcement learning: An introduction*. Cambridge, MA: MIT press, 2018.
- [22] C. A. Cheng, "Efficient and principled robot learning: theory and algorithms," Ph.D. dissertation, School of Interactive Computing, Georgia Institute of Technology, Atlanta, GA, 2020.
- [23] P. Abbeel and A. Y. Ng, "Exploration and apprenticeship learning in reinforcement learning," in *Proceedings of International Conference on Machine Learning*, 2005, pp. 1–8.
- [24] S. Ross and D. Bagnell, "Efficient reductions for imitation learning," in *Proceedings of International Conference on Artificial Intelligence and Statistics*, 2010, pp. 661–668.
- [25] S. Ross, G. Gordon, and D. Bagnell, "A reduction of imitation learning and structured prediction to no-regret online learning," in *Proceedings of International Conference on Artificial Intelligence and Statistics*, 2011, pp. 627–635.
- [26] K.-W. Chang *et al.*, "Learning to search better than your teacher," in *Proceedings of International Conference on Machine Learning*. PMLR, 2015, pp. 2058–2066.
- [27] H. M. Le *et al.*, "Hierarchical imitation and reinforcement learning," in *Proceedings of International Conference on Machine Learning*, 2018.
- [28] W. Sun, "Towards generalization and efficiency in reinforcement learning," Ph.D. dissertation, The Robotics Institute, Carnegie Mellon University, Pittsburgh, PA, 2019.
- [29] G. Brockman *et al.*, "Openai gym," 2016.
- [30] Z. Wang *et al.*, "Coordinated energy management of networked microgrids in distribution systems," *IEEE Trans. Smart Grid*, vol. 6, no. 1, pp. 45–53, 2015.
- [31] R. A. Jabr, R. Singh, and B. C. Pal, "Minimum loss network reconfiguration using mixed-integer convex programming," *IEEE Trans. Power Syst.*, vol. 27, no. 2, pp. 1106–1115, 2012.
- [32] M. Baran and F. Wu, "Network reconfiguration in distribution systems for loss reduction and load balancing," *IEEE Trans. Power Deliv.*, vol. 4, no. 2, pp. 1401–1407, apr 1989.
- [33] W. E. Hart *et al.*, *Pyomo-optimization modeling in python*, 2nd ed. Springer Science & Business Media, 2017, vol. 67.